

## Pulmonary toxicity of inhaled nano-sized cerium oxide aerosols in Sprague–Dawley rats

Chang Guo<sup>a</sup>, Sarah Robertson<sup>a</sup>, Ralf J. M. Weber<sup>b</sup>, Alison Buckley<sup>a</sup>, James Warren<sup>a</sup>, Alan Hodgson<sup>a</sup>, Joshua Z. Rappoport<sup>c</sup>, Konstantin Ignatyev<sup>d</sup>, Kirsty Meldrum<sup>a</sup>, Isabella Römer<sup>a</sup>, Sameirah Macchiarulo<sup>a</sup>, James Kevin Chipman<sup>b</sup>, Tim Marczylo<sup>a</sup>, Martin O. Leonard<sup>a</sup>, Timothy W. Gant<sup>a</sup>, Mark R. Viant<sup>b</sup> and Rachel Smith<sup>a</sup>

<sup>a</sup>Centre for Radiation, Chemical and Environmental Hazards, Public Health England, Harwell Science and Innovation Campus, Didcot, Oxfordshire, OX11 0RQ, UK; <sup>b</sup>School of Biosciences, University of Birmingham, Birmingham, B15 2TT, UK; <sup>c</sup>Department of Cell and Molecular Biology, Northwestern University, Chicago, IL, USA; <sup>d</sup>Diamond Light Source Ltd, Harwell Science and Innovation Campus, Didcot, Oxfordshire, OX11 0DE, UK

### ABSTRACT

Cerium oxide nanoparticles (CeO<sub>2</sub>NPs), used in some diesel fuel additives to improve fuel combustion efficiency and exhaust filter operation, have been detected in ambient air and concerns have been raised about their potential human health impact. The majority of CeO<sub>2</sub>NP inhalation studies undertaken to date have used aerosol particles of larger sizes than the evidence suggests are emitted from vehicles using such fuel additives. Hence, the objective of this study was to investigate the effects of inhaled CeO<sub>2</sub>NP aerosols of a more environmentally relevant size, utilizing a combination of methods, including untargeted multi-omics to enable the broadest possible survey of molecular responses and synchrotron X-ray spectroscopy to investigate cerium speciation. Male Sprague–Dawley rats were exposed by nose-only inhalation to aerosolized CeO<sub>2</sub>NPs (mass concentration 1.8 mg/m<sup>3</sup>, aerosol count median diameter 40 nm) for 3 h/d for 4 d/week, for 1 or 2 weeks and sacrificed at 3 and 7 d post-exposure. Markers of inflammation changed significantly in a dose- and time-dependent manner, which, combined with results from lung histopathology and gene expression analyses suggest an inflammatory response greater than that seen in studies using micron-sized ceria aerosols. Lipidomics of lung tissue revealed changes to minor lipid species, implying specific rather than general cellular effects. Cerium speciation analysis indicated a change in Ce<sup>3+</sup>/Ce<sup>4+</sup> ratio within lung tissue. Collectively, these results in conjunction with earlier studies emphasize the importance of aerosol particle size on toxicity determination. Furthermore, the limited effect resolution within 7 d suggested the possibility of longer-term effects.

### ARTICLE HISTORY

Received 3 July 2018  
Revised 27 November 2018  
Accepted 28 November 2018





### KEYWORDS


Nanoparticle; cerium; omics; rat; inhalation

## Introduction

Nanomaterials offer unique mechanical, chemical, electrical and optical properties that are being exploited for an extensive range of applications; however, concerns remain about their potential impact on human health. Cerium oxide nanoparticles (CeO<sub>2</sub>NPs) are one of the manufactured nanomaterials currently receiving significant attention with respect to their potential health risks as they are used in a range of applications with the

potential for direct human exposure, including polishing media (Reed et al. 2014) and fuel-borne catalysts, such as Eolys<sup>TM</sup>, Platinum Plus<sup>TM</sup>, and Envirox<sup>TM</sup> (Majestic et al. 2010). The benefits of CeO<sub>2</sub>NP-based fuel additives include reduced emissions of gaseous products of incomplete combustion and improved fuel combustion efficiency (Zhang et al. 2013). However, CeO<sub>2</sub>NPs have been detected in ambient air in locations where such additives are in use (Park et al. 2008a, Gantt et al. 2015) and there are concerns about their potential

**CONTACT** Chang Guo  [chang.guo@phe.gov.uk](mailto:chang.guo@phe.gov.uk)  Centre for Radiation, Chemical and Environmental Hazards, Public Health England, Harwell Science and Innovation Campus, Didcot, Oxfordshire, OX11 0RQ, UK; Rachel Smith  [rachel.smith@phe.gov.uk](mailto:rachel.smith@phe.gov.uk)  Centre for Radiation, Chemical and Environmental Hazards, Public Health England, Harwell Science and Innovation Campus, Didcot, Oxfordshire, OX11 0RQ, UK

 Supplemental data for this article can be accessed [here](#).

Color versions of one or more of the figures in the article can be found online at [www.tandfonline.com/inan](http://www.tandfonline.com/inan).

This article has been republished with minor changes. These changes do not impact the academic content of the article.

© 2019 Crown Copyright. Reproduced with the permission of Public Health England. Published by Informa UK Limited, trading as Taylor & Francis Group  
This is an Open Access article distributed under the terms of the Creative Commons Attribution-NonCommercial-NoDerivatives License (<http://creativecommons.org/licenses/by-nc-nd/4.0/>), which permits non-commercial re-use, distribution, and reproduction in any medium, provided the original work is properly cited, and is not altered, transformed, or built upon in any way.

impact on health following inhalation (Geraets et al. 2012).

Reported effects of CeO<sub>2</sub>NPs *in vivo* following intratracheal instillation include alveolar epithelial hyperplasia, lung inflammation, air-blood barrier damage, and fibrosis of the lungs (Ma et al. 2011; Ma et al. 2012; Peng et al. 2014; Rice et al. 2015). A number of *in vivo* inhalation studies have also reported similar effects, with indications that pulmonary inflammatory responses are slow to resolve post-exposure (Aalapati et al. 2014). Inhalation bio-distribution studies have also found significant accumulation in pulmonary tissue and slow clearance (Geraets et al. 2012; Li et al. 2016).

Field studies have identified ceria particles emitted from vehicles using the Envirox™ fuel additive, with a size range from 5 to 100 nm (Gantt et al. 2014). However, to date, the majority of reported CeO<sub>2</sub>NP inhalation studies, as summarized in Table 1, including those mentioned above, have used aerosols in the micron-size range or at the upper end of the nano-size range and therefore, given the importance of particle size in driving biological effects (Oberdörster, Ferin, & Lehnert 1994; Braakhuis et al. 2016), may not be directly relevant to a hazard assessment of the effect of ceria particles emitted from engines using CeO<sub>2</sub>NP fuel additives. The purpose of this study was, therefore, to undertake a short-term *in vivo* inhalation study using a ceria aerosol with a more environmentally relevant aerosol particle size, to investigate the effects on lung inflammation and injury. It was anticipated that comparing the results of this study with those in the literature, which have all used significantly larger aerosol particle sizes, would provide support for the hypothesis that aerosol particle size is an important toxicity driver.

We also utilized a multi-omics approach – applying microarray-based gene expression profiling and untargeted mass spectrometry-based lipidomics – to enable a broad measurement of thousands of molecular endpoints to provide insights into the toxicity mechanisms of CeO<sub>2</sub>NPs (Taylor et al. 2016; Dekkers et al. 2018). Furthermore, we assessed the distribution of inhaled CeO<sub>2</sub>NPs in various organs and their physicochemical properties using a range of approaches. Many studies have indicated that the physicochemical properties of nanomaterials have a significant influence on their biological

activity. CeO<sub>2</sub>NPs are an interesting case as it has been hypothesized that initial differences in the Ce<sup>3+</sup>/Ce<sup>4+</sup> ratio on the NP surface, and changes in their anti-oxidant potential following exposure, may play a significant role in toxicity determination (Auffan et al. 2009). To explore this, synchrotron-based spectroscopy was applied to determine cerium oxidation states in exposed lung tissues.

## Materials and methods

### Cerium oxide nanoparticles

CeO<sub>2</sub>NPs (primary particle size 8 nm) were provided by the University of Birmingham. Details of the synthesis are described in the [Supplementary information](#) (Chen et al. 2013). The powder was dispersed in MilliQ water (1 mg/mL) and sonicated briefly (~ 1 min) prior to use.

### Exposure system and aerosol characterization

The nose-only inhalation exposure system and the aerosol characterization undertaken are described in the [Supplementary information](#). Details of the dose estimation method are also described in the [Supplementary information](#).

### Study design

The experiments were performed within the legal framework of the United Kingdom under a Project License granted by the Home Office of Her Majesty's Government. All procedures involving the animals were performed in accordance with the Animals (Scientific Procedures) Act 1986. Male Sprague–Dawley (SD) rats (10–12 weeks, 250–320 g) were purchased from Harlan, UK. Rats were randomly assigned into groups and exposed to aerosolized CeO<sub>2</sub>NPs or water (controls) for 3 h per day, for 4 d per week, for 1 or 2 weeks. The 2-week exposure was chosen to explore the effect of a higher deposited dose within the lung, an alternative approach of using a higher aerosol concentration was discounted as this would have affected the aerosol particle size. Following exposure, the rats were returned to their cages for a period of either 3 d, to characterize the initial response, or 7 d to explore recovery and other effects in the short-

term. Assessment of adverse clinical signs is described in the [Supplementary information](#).

### **Analysis of bronchoalveolar lavage fluid (BALF)**

Rats were sacrificed by exsanguination by cardiac puncture under isoflurane anesthesia (induced at 5%, maintained at 1.5–2% in 100% oxygen). Bronchoalveolar lavage was performed *in situ* via tracheal cannula with  $2 \times 7$  mL aliquots of phosphate buffered saline (PBS). Cells from both aliquots were pooled for cytological analysis as described in the [Supplementary information](#). BALF supernatants from the first wash were collected for analysis of cytotoxicity and alveolar barrier damage as described in the [Supplementary information](#).

Cytokines and chemokines including IL-1 $\beta$  (interleukin-1 $\beta$ ), TNF- $\alpha$  (tumor necrosis factor- $\alpha$ ), TGF- $\beta$ 1 (transforming growth factor- $\beta$ 1), CXCL2 (CINC-3, cytokine-induced neutrophil chemoattractant 3), CXCL1 (CINC-1, cytokine-induced neutrophil chemoattractant 1), and CCL2 (MCP-1, monocyte chemoattractant protein-1) were measured in BALF supernatants using R&D Systems Quantikine<sup>®</sup> ELISA kits according to the manufacturer's specifications.

### **Lung tissue processing**

Following lavage, the apical and azygous lung lobes were tied off and snap frozen in liquid nitrogen for multi-omics analysis. The remainder of the lungs was removed and inflated and fixed with freshly made 4% paraformaldehyde via tracheal cannula, at a pressure of 30 cm of water and then processed into paraffin blocks. Cross/transverse sections of lung tissues chosen randomly were cut at a thickness of 5  $\mu$ m before mounting onto microscope slides. For histopathology, staining with hematoxylin and eosin (H&E) was performed on lung tissue sections.

### **Multi-omics analysis of lung**

Lung tissues were homogenized in 8 mL/g (v/w wet mass) methanol and 2.5 mL/g (v/w) water using a bead-based homogenizer (Precellys 24; Stretton Scientific, Stretton, UK). Lung homogenate aliquots were then taken for both metabolite and RNA extractions. Total RNA was isolated using Qiagen's mini RNeasy Kit and QIAshredder (Qiagen, Crawley,

UK) according to the manufacturer's protocol. RNA was quantified with a NanoDrop 1000 spectrophotometer (Thermo Scientific, Waltham, MA), and the integrity of RNA was verified with a 2100 Bioanalyzer (Agilent Technologies, Santa Clara, CA). Lipids from the lung homogenate were extracted using a methanol:water:chloroform (2:2:1.8) solvent system (Wu et al. 2008), dried using a centrifugal concentrator and stored at  $-80^{\circ}\text{C}$  until analysis.

Microarray-based gene expression profiling was performed according to the manufacturer's protocol (Agilent Technologies, Santa Clara, CA). Further details are described in the [Supplementary information](#). Mass spectrometry-based lipidomics was performed using a high-resolution spectral-stitching nanoelectrospray direct-infusion approach as previously reported (Southam et al. 2017). Further details are described in the [Supplementary information](#).

### **Cerium in tissues determined by ICP-MS and laser ablation ICP-MS**

The cerium content of liver and kidney samples was determined using inductively coupled plasma mass spectrometry (ICP-MS) as described in the [Supplementary information](#). Elemental mapping of cerium in lung tissue samples was undertaken by laser ablation ICP-MS using a New Wave Research NWR213 laser ablation system (Electro Scientific Industries, Portland, OR) linked to an iCAP Q ICPMS (Thermo Fisher Scientific, Hemel Hempstead, UK). Further details are described in the [Supplementary information](#).

### **Transmission electron microscopy (TEM)**

Lung tissues from animals at 3 d after 2-week exposure (CeO<sub>2</sub>NP exposed and control) were prepared as described in the [Supplementary information](#) and TEM imaging was then performed using an FEI Tecnai Spirit G2.

### **Synchrotron-based X-ray spectroscopy**

Synchrotron microfocus X-ray spectroscopy was carried out at the Diamond Light Source I18 Beamline (Oxfordshire, UK). Microfocus X-ray fluorescence ( $\mu$ -XRF) analysis was undertaken to provide information on the spatial distribution of elements of interest for a number of lung sections. For identified areas of high cerium concentration, X-ray

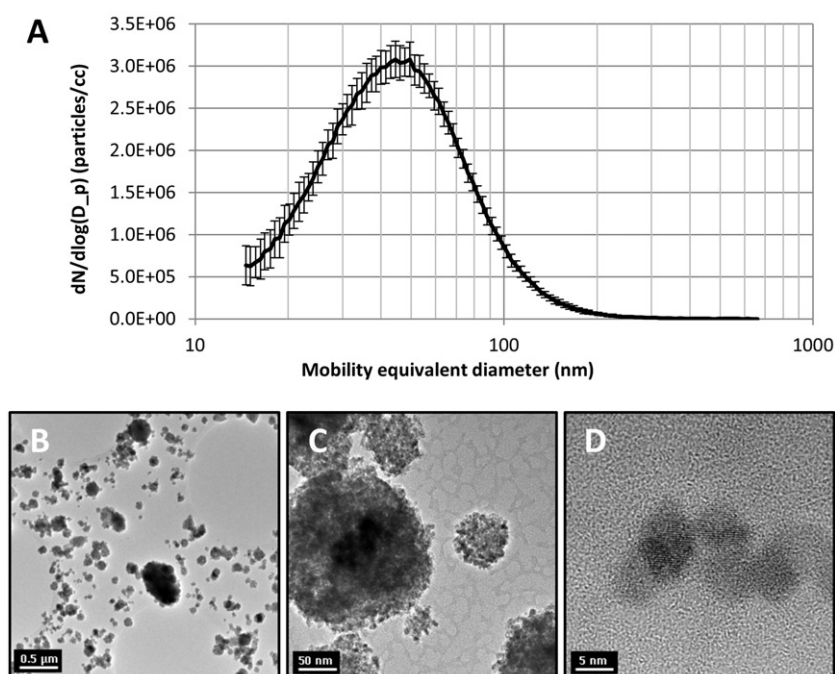


**Figure 1.** (A) CeO<sub>2</sub>NP aerosol particle size distribution. (B–D) Transmission electron microscope images of CeO<sub>2</sub>NP aerosol particles illustrating clear crystalline form (D).

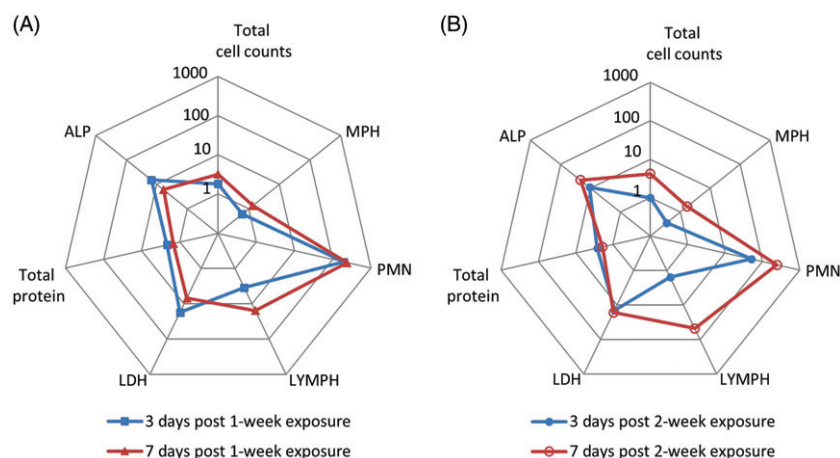


**Figure 2.** Comparison of changes in BALF parameters after 1 week (A) and 2 weeks (B) of exposure to CeO<sub>2</sub>NP aerosols. Changes are shown as fold differences compared to controls (H<sub>2</sub>O aerosols) using logarithmic scaling (MPH: macrophages; PMN: neutrophils; LYMPH: lymphocytes; LDH: lactate dehydrogenase; ALP: alkaline phosphatase).

absorption near-edge structure (XANES) spectrometry of the Ce L<sub>III</sub>-edge was carried out to investigate chemical speciation (e.g. oxidation state). The spectra produced were compared with those for samples of some cerium compounds: Ce<sub>2</sub>(CO<sub>3</sub>)<sub>3</sub>, Ce(OH)<sub>4</sub> (Sigma-Aldrich, St. Louis, MO), and CeO<sub>2</sub> (Acros Organics, Morris, NJ), and a sample of the CeO<sub>2</sub>NPs. Further details are described in the [Supplementary information](#).

## Results

### Aerosol characterization

Aerosol characteristics and lung dose estimates are presented in [Table 2](#) and [Figure 1](#), including representative images of agglomerated CeO<sub>2</sub>NP aerosol particles, illustrating their spherical form and primary particle size consistent with the manufacturer's data (ca 8 nm) (Chen et al. 2013).



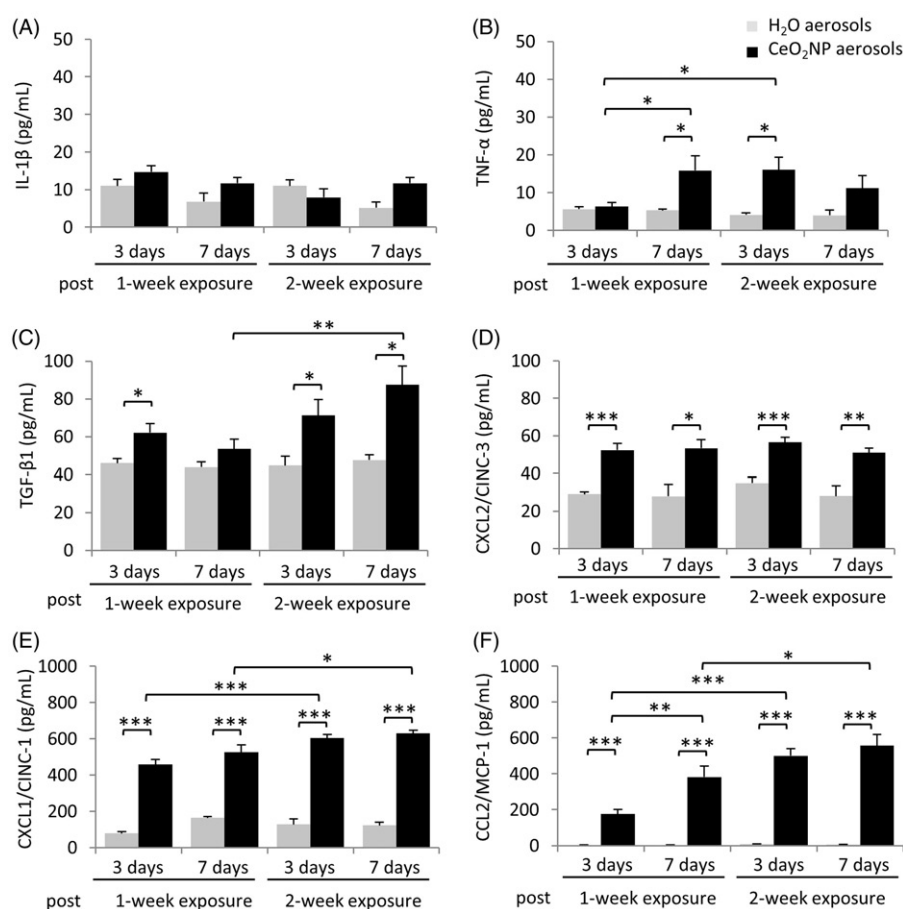


**Figure 3.** Cytokine levels in BALF from rats exposed to H<sub>2</sub>O or CeO<sub>2</sub>NP aerosols. (A) IL-1 $\beta$ , (B) TNF- $\alpha$ , (C) TGF- $\beta$ 1, (D) CXCL2/CINC-3, (E) CXCL1/CINC-1, and (F) CCL2/MCP-1. Data shown as mean  $\pm$  SD ( $n = 5$  rats for groups exposed to CeO<sub>2</sub>NP aerosols and  $n = 3$  for control groups exposed to H<sub>2</sub>O aerosols). \*  $p < 0.05$ , \*\*  $p < 0.01$ , \*\*\*  $p < 0.001$ .

### Acute pulmonary toxicity effects induced by inhaled CeO<sub>2</sub>NPs

Inhalation exposure to CeO<sub>2</sub>NPs did not affect the body weight development of the rats (data not shown). No adverse clinical signs were observed in any of the animals.

### Cytology and cytotoxicity analysis of bronchoalveolar lavage fluid (BALF)

BALF analysis was undertaken at 3 d and 7 d post-exposure for both 1-week and 2-week exposure groups. The majority of BALF parameters showed significant increases for CeO<sub>2</sub>NP exposed groups compared to the control groups (Figure 2, with details presented in Supplementary Figures S2 and S3). For the 1-week exposure group, there was a small but significant increase in the different cell populations between 3 and 7 d post-exposure, although the levels of total protein, lactate dehydrogenase (LDH) and alkaline phosphatase (ALP) showed a reduction over

this period indicating limited recovery. For the 2-week exposure group, there was no significant change in the total protein, LDH or ALP levels between 3 and 7 d post-exposure, but significant increases in the different cell populations. The above indicates that the inhaled CeO<sub>2</sub>NPs induced time- and dose-dependent inflammation and lung damage.

### Cytokines/chemokines in BALF

Effects on several cytokines and chemokines relevant to inflammatory responses and allergic effects were considered. There was no significant change in IL-1 $\beta$  concentrations for any exposed group (Figure 3(A)), whereas for TNF- $\alpha$  and TGF- $\beta$ 1 there were significant increases in some groups (Figure 3(B,C)). For CXCL2, CXCL1, and CCL2, there were significant increases for all exposed groups (Figure 3(D-F)). The effects were the greatest for CXCL1 and CCL2, for which there was a clear dose-dependent effect at both post-exposure times. There was also some indication of

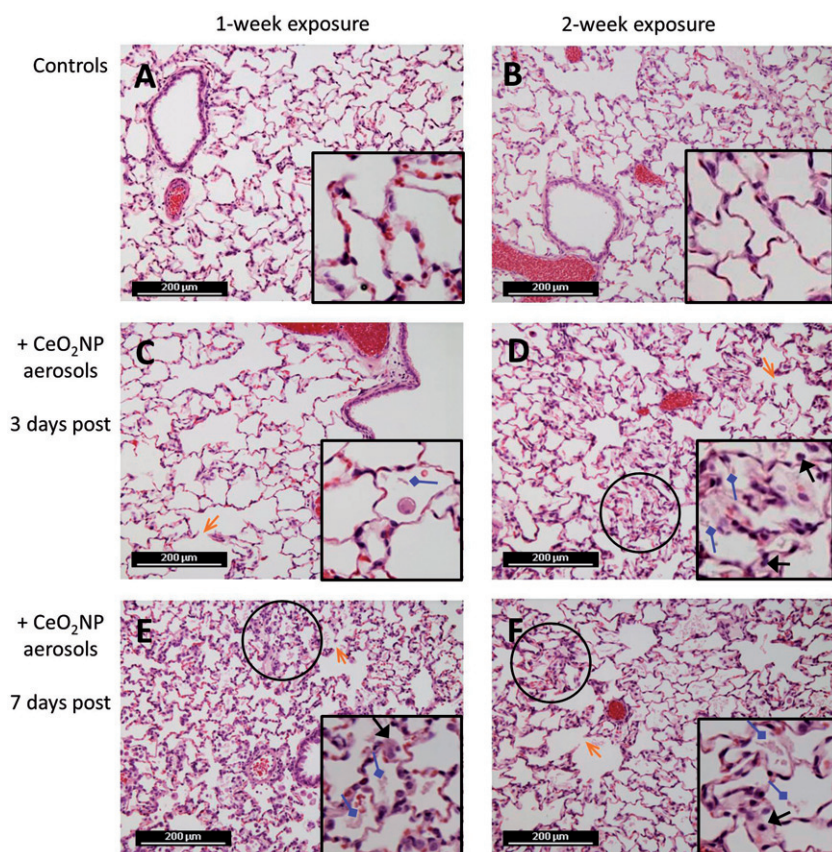


**Figure 4.** Representative hematoxylin and eosin stained lung sections ( $\times 200$ , inset  $\times 400$ ) from rats of negative controls (A and B) and  $\text{CeO}_2\text{NP}$  aerosol exposure at 3 d (C and D) and 7 d (E and F) post-exposure (A, C, E, 1-week exposure; B, D, F, 2-week exposure). Symbols indicate some histopathological observations including infiltration of inflammatory cells (black arrows), deposition of amorphous eosinophilic materials (diamond arrows), alveolar wall injury (open arrows) and minor alveolar epithelial hyperplasia (areas inside black circles).

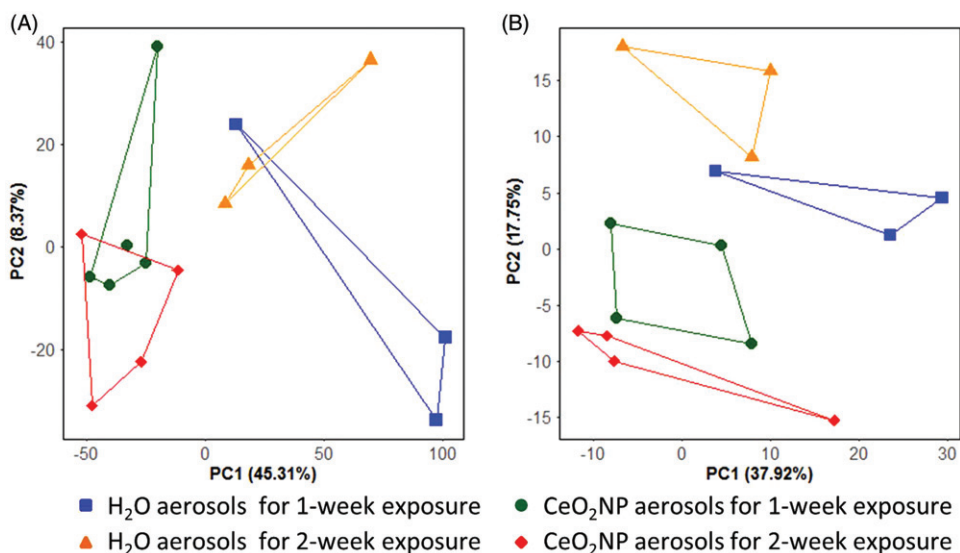


**Figure 5.** Principal component analysis (PCA) score plots of the gene expression (A) and lipidomics profiles (B) of lung tissue from rats exposed to  $\text{H}_2\text{O}$  and  $\text{CeO}_2\text{NP}$  aerosols for 1 week and 2 weeks at 3 d post-exposure.

concentrations increasing with time post inhalation, although this was only significant for  $\text{CCL2}$  for the 1-week exposure. For the others, patterns were less

clear, with  $\text{CXCL2}$  showing no dose- or time-dependence,  $\text{TGF-}\beta 1$  showing no time-dependence and dose-dependence for the 7-d groups only, and  $\text{TNF-}\alpha$

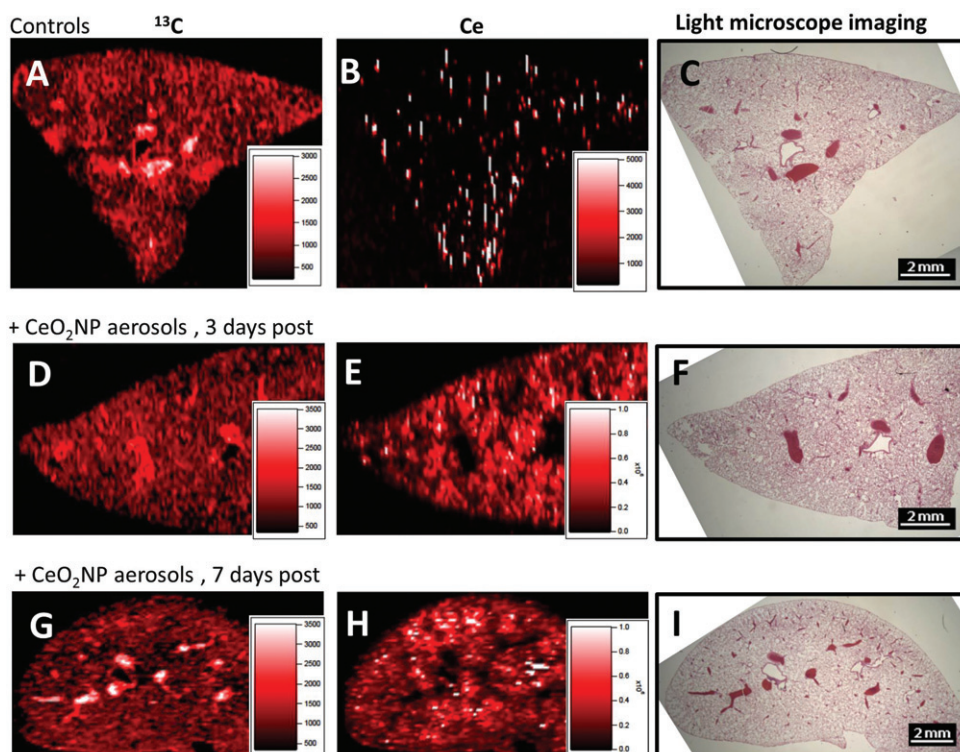


**Figure 6.** Representative laser ablation inductively coupled plasma mass spectrometry elemental maps (isotopes  $^{13}\text{C}$  and  $^{140}\text{Ce}$ ) and light microscopy images ( $\times 12.5$ ) of lung tissues of negative controls (images A–C) and  $\text{CeO}_2\text{NP}$  aerosol exposed animals at 3 days (images D–F) and 7 d (images G–I) post-exposure. The light microscope images show the lung tissue section prior to undertaking laser ablation (which destroys the sample) and allow the overall shape and structures such as large airways and larger blood vessels to be seen for comparison purposes.

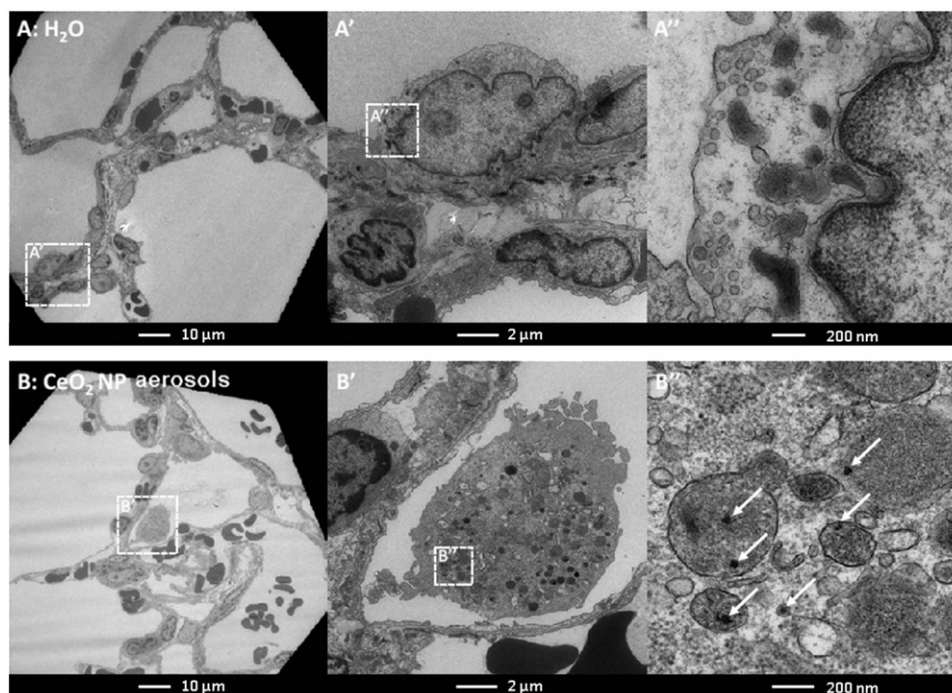


**Figure 7.** Transmission electron microscope images of lung tissue from rats exposed to  $\text{H}_2\text{O}$  aerosols (A) and  $\text{CeO}_2\text{NP}$  aerosols (B) for 2 weeks at 3 d post-exposure. The boxes with dotted lines denote the approximate locations of the corresponding magnified regions.



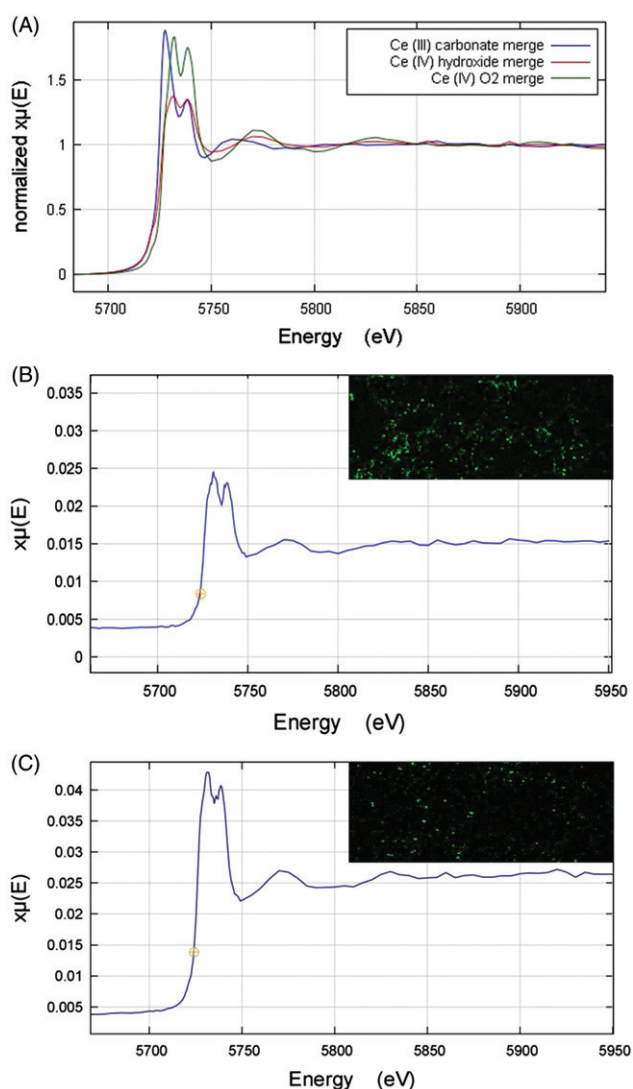


**Figure 8.** (A) XANES Ce  $L_{III}$  spectra for cerium standard samples of  $Ce_2(CO_3)_3$ ,  $Ce(OH)_4$ , and  $CeO_2$ . (B–C) XANES Ce  $L_{III}$  spectra derived from cerium-rich pixels of elemental  $\mu$ -XRF maps of lung tissue sections from rats exposed to the  $CeO_2$ NP aerosols for two weeks at 3 d (B, A combination of 4 pixels) and 7 d (C, A combination of 6 pixels) post-exposure. The top right-hand corner images in B and C are the associated elemental  $\mu$ -XRF maps of cerium in lung tissue samples from animals post-exposure. Data obtained using the I18 beamline at the Diamond Light Source (pixel size  $4 \mu m \times 4 \mu m$ ).

showing dose-dependence for the 3-d groups only and time-dependence for the 1-week exposure groups only.

### Histopathology – lung inflammatory changes

Inhalation of  $CeO_2$ NPs resulted in mild inflammation for both exposure durations and at both 3 and 7 d post-exposure (Figure 4). The lung architecture was

well preserved with inhaled  $CeO_2$ NPs but minor alveolar epithelial hyperplasia with accumulation of eosinophilic materials from macrophage breakdown was observed. The lung injury induced by  $CeO_2$ NPs appeared to increase with time for 1-week exposure based on the histopathological observations.

### Multi-omics analysis of lung

Principal component analysis (PCA) score plots from the analysis of the gene expression and lipidomics measurements are shown in Figure 5. For the gene expression analysis, the score plot captured 53.6% of the variation in the dataset within the first two components; a significant separation between rats exposed to  $H_2O$  aerosols and  $CeO_2$ NP aerosols was discovered along PC1 ( $t$ -test of the scores values:  $p = 4.0 \times 10^{-3}$ , Figure 5(A)), confirming that the NP exposure induced perturbations to gene transcription. The PCA score plot derived from the lipidomics data captured 55.6% of the variation in the first two components, and also showed a significant separation between control and  $CeO_2$ NP aerosols, in this case along PC2 ( $t$ -test of the scores values:  $p = 8.5 \times 10^{-4}$ , Figure 5(B)). Limma was applied to the gene expression data to investigate the effects of  $CeO_2$ NP exposure ( $H_2O$  aerosol exposure as the controls) and it was found to be statistically significant with  $CeO_2$ NP exposure ( $q < 0.05$  and  $\log_2$ -fold change  $> 1.0$ ) for 67 genes (Supplementary Table S1). DAVID analysis on the 67 differentially expressed genes (of which 53 were matched to a gene present in DAVID) yielded 13 GO-categories that were significantly enriched ( $q < 0.05$ , Supplementary Table S2).

For the lipidomics data, two-way ANOVA (type II, unbalanced) was conducted on each peak to investigate the effects of inhaled  $CeO_2$ NPs and exposure dose (1-week versus 2-week exposure).  $CeO_2$ NP inhalation was statistically significant for 38 peaks ( $q < 0.05$ ) of which 19 were putatively annotated with a lipid name from the Lipid Maps database (Supplementary Table S3 and Supplementary File S11). Exposure dose had no significant effect on any of the peak intensities. Enrichment analysis of categorical annotations of the significant and annotated lipids was conducted, using MBROLE (Lopez-Ibanez, Pazos, & Chagoyen 2016) (Supplementary Table S4) and LIPID Metabolites And Pathways Strategy (LIPID



MAPS<sup>®</sup>), and revealed that several lipid classes (e.g. glycerophospholipids) and subclasses (e.g. diacylglycerophosphocholines, glycerophosphoethanolamines, and diacylglycerophosphoethanolamines) were significantly enriched.

### **Assessment of the inhaled CeO<sub>2</sub>NPs**

#### **Detection of CeO<sub>2</sub>NPs deposited in the lung**

Elemental maps of lung tissues produced by laser ablation ICP-MS clearly indicate the presence of cerium, widely distributed within the lung lobes, without any significant association with the larger airways or larger blood vessels (Figure 6). TEM micrographs (Figure 7) indicate the presence of dense particle agglomerates of similar size to the CeO<sub>2</sub>NP aerosol agglomerates in the alveolar macrophages, mainly in the lysosome-like intracellular vesicles.

#### **Cerium in liver and kidney**

The concentrations of cerium in the liver and kidney were measured by ICP-MS and were greater in exposed than control animals, higher for 2-week than 1-week exposure, and increased from 3 d to 7 d post-exposure, indicating the translocation of cerium from the lung to other organs after inhalation, however, these changes were only statistically significant for some groups (Supplementary Figure S5).

#### **Cerium speciation by synchrotron X-ray spectroscopy**

Cerium L<sub>III</sub> XANES spectra of the cerium compounds Ce<sub>2</sub>(CO<sub>3</sub>)<sub>3</sub>, CeO<sub>2</sub>, and Ce(OH)<sub>4</sub> are shown in Figure 8(a). Both Ce<sup>4+</sup> compounds (CeO<sub>2</sub>, and Ce(OH)<sub>4</sub>) show a doublet peak of roughly equal height, whereas the Ce<sup>3+</sup> carbonate (Ce<sub>2</sub>(CO<sub>3</sub>)<sub>3</sub>) shows a clearly different peak morphology. The XANES spectrum for the CeO<sub>2</sub>NP sample appears qualitatively similar to the Ce<sup>4+</sup> compounds (Supplementary Figure S6). A linear combination fitting (LCF) analysis was carried out for the CeO<sub>2</sub>NP spectrum using the spectra from the cerium compounds as standards. The fit analysis indicated that the CeO<sub>2</sub>NP sample was 100% CeO<sub>2</sub> with zero contributions from the other standards.

Cerium mapping of lung tissue sections from exposed rats was undertaken using  $\mu$ -XRF, and XANES spectra collected from identified areas of high cerium concentration (Figure 8(B,C)). Quantitative LCF analysis was carried out in each case, using the standards' spectra. The results indicated 21% Ce<sup>3+</sup> carbonate and 79% Ce<sup>4+</sup> oxide at 3 d and 15% Ce<sup>3+</sup> carbonate and 85% Ce<sup>4+</sup> oxide at 7 d post-exposure. In comparison to the ~100% Ce<sup>4+</sup> in the aerosol NPs, these results indicate changes to cerium speciation in the lung following inhalation; however, given the limited sample numbers, it is not possible to judge whether the difference between 3 and 7 d is significant.

### **Discussion**

We have investigated the pulmonary toxicity of nano-sized CeO<sub>2</sub>NP aerosol agglomerate particles (CMD approximately 40 nm, GSD 1.7; primary particle size 5–10 nm). Histopathology indicated mild inflammation with alveolar epithelial hyperplasia (Figure 4), which increased with time after exposure, suggesting the potential for long-term effects. Consistent with this the BALF analysis indicates a significant inflammatory response increasing between 3 and 7 d (Figure 2 and Supplementary Figure S2 and S3). These changes were matched by significant increases in cytokines involved in inflammatory cell infiltration, such as CXCL1(CINC-1) and CCL2(MCP-1) (Figure 3), with levels increasing with dose for each post inhalation time (dose-dependence). Concentrations of total protein, LDH, and ALP in BALF increased significantly for all groups exposed to CeO<sub>2</sub>NP aerosols (Figure 2 and Supplementary Figure S3) with some evidence of recovery only for the 1-week exposures, again suggesting the potential for longer-term effects. The gene expression results (Supplementary Table S2) are consistent with the above, with significant Gene Ontology terms including (GO:0030593) neutrophil chemotaxis, (GO:0048247) lymphocyte chemotaxis, (GO:0008009) chemokine activity, and (GO:0002548) monocyte chemotaxis.

Other CeO<sub>2</sub>NP inhalation studies have also shown lung inflammation, cytotoxicity, and air-blood barrier damage; however, the majority of such studies have used aerosols with micron-sized aerosol

Table 1. Summary of inhalation toxicity studies with CeO<sub>2</sub>NPs.

CeO <sub>2</sub> particles	Characterization of primary particles			Exposure dose (aerosol concentration × exposure duration)	Animal models	Animal sacrifice time points post-exposure	Brief biological findings	Reference (* nose-only inhalation; ** whole-body exposure)
	Primary particle diameter (nm)	Surface area (m <sup>2</sup> /g)	Characterization of aerosols (MMAD – mass median aerodynamic diameter; GSD – geometric standard deviation; CMD – count median diameter; GMD – geometric mean diameter)					
CeO <sub>2</sub> NPs (NanoAmorph)	15-30 (manufacturer), 55 (SEM)	30-50 (manufacturer)	MMAD (μm)/GSD 2.28/2.94	641 mg/m <sup>3</sup> × 4 hrs	Wistar rats	1, 2 and 14 d post	Significant cytotoxicity, oxidative stress and inflammation in the lungs.	(Srinivas et al.,2011) *
CeO <sub>2</sub> NPs (NM-211) (Antaria);	5-10 (manufacturer), 13.0 ± 3.2 (TEM), 44.9 ± 14.6 (SEM); 211)	63.95 ± 0.30;	MMAD (μm)/GSD 1.02 ± 0.04/1.82;	10.79 ± 0.82 mg/m <sup>3</sup> × 40 min/ Wistar rats d, 2 h/d or 6 h/d × 1 d or 5 d/wk × 2 wks or 4 wks;	Wistar rats	6 h/d groups only - 1 d post plus 2/3 d post the 4-wk exposure groups	There was no clear effect of the primary particle size or surface area on pulmonary deposition and extrapulmonary tissue distribution.	(Geraets et al.,2012) *
CeO <sub>2</sub> NPs (NM-212) (Umicore);	40 (manufacturer), 27.3 ± 13.6 (TEM), 28.4 ± 10.4 (SEM);	27.15 ± 0.19;	MMAD (μm) /GSD 1.17 ± 0.34/2.07;	19.95 ± 13.21 mg/m <sup>3</sup> × 40 min/d, 2 h/d or 6 h/d × 1 d or 5 d/wk × 2 wks or 4 wks;	Wistar rats	4-wk groups only - 1 d post all exposure groups, and 28 d post the 6 h/d groups	All three materials gave rise to similar levels of pulmonary inflammation, with dose-dependent increases in total cell numbers, macrophages, neutrophils and lymphocytes in BALF. Systemic effects were virtually absent.	(Gosens et al.,2014) *
CeO <sub>2</sub> (NM-213) (Sigma)	<5000 (manufacturer), 615.3 ± 430.5 (SEM)	3.73 ± 0.01;	MMAD (μm) /GSD 1.40 ± 0.11/1.64	55.00 ± 6.2 mg/m <sup>3</sup> × 40 min/d, 2 h/d or 6 h/d × 1 d or 5 d/wk × 2 wks or 4wks	Sprague-Dawley rats	1 d post	Exposure to uncoated CeO <sub>2</sub> NPs caused lung injury and inflammation with increased PMN and LDH levels in the BALF of the rats, whereas exposure to SiO <sub>2</sub> -coated CeO <sub>2</sub> NPs did not induce any pulmonary toxicity.	(Demokritou et al.,2013) **
CeO <sub>2</sub> NPs (uncoated) (produced in-house);	17.3 (XRD), 12.8 (BET equivalent diameter);	61;	CMD (nm)/GSD 1.55 ± 0.05; MMAD (nm)/GSD 281/3.09;	2.7 mg/m <sup>3</sup> × 2 h/d × 4 d	Sprague-Dawley rats	1 d post	Exposure to uncoated CeO <sub>2</sub> NPs caused lung injury and inflammation with increased PMN and LDH levels in the BALF of the rats, whereas exposure to SiO <sub>2</sub> -coated CeO <sub>2</sub> NPs did not induce any pulmonary toxicity.	(Aalapati et al.,2014) *
SiO <sub>2</sub> -coated CeO <sub>2</sub> NPs (produced in-house)	21 (XRD), 19.2 (BET equivalent diameter)	50	CMD (nm)/GSD 100.4 ± 5.2/1.481 ± 0.006, MMAD (nm)/GSD 341/5.02	2.0 ± 0.035 mg/m <sup>3</sup> × 6 h/d × CD1 rats 0, 7, 14, 28 d	Wistar rats	1 d post all exposure groups, and 14 and 28 d post 28-d exposure group	Inhalation exposure of CeO <sub>2</sub> NPs induced significant pulmonary and some extrapulmonary toxicity.	(Landsiedel et al.,2014) *
CeO <sub>2</sub> NPs (NanoAmorph)	15-30 (manufacturer), 45 (TEM)	30-50 (manufacturer), 56 ± 25 (BET)	MMAD (μm)/GSD 0.6/2.4, 0.9/2.3, 0.8/2.5;	0.8, 3.0, 11.6 mg/m <sup>3</sup> × 6 h/d Wistar rats × 5 d;	Wistar rats	3 and 24 d post for all exposure groups	Inhaled CeO <sub>2</sub> NPs and Al-doped CeO <sub>2</sub> NPs caused a transient, concentration-dependent inflammation of the lung at all concentrations.	(Landsiedel et al.,2014) *
CeO <sub>2</sub> NPs (NanoCare project);	0-200 (TEM), > 10 × 10 <sup>3</sup> (SEM), 36 (XRD);	33.0;	MMAD (μm)/GSD 1.3/2.1, 2.2/1.9, 2.4/2.1	0.6, 2.1, 9.2 mg/m <sup>3</sup> × 6 h/d × 5 d	Wistar rats	1-wk groups - BALF at 3 and 24 d post and histopathology and organ burden at 0 and 21 d post. 4-wk groups - BALF 1 and 35 d post, histopathology at 2 and 34 d post and lung burden at 7 time points to exposures 129 d post	Inhaled CeO <sub>2</sub> NPs cleared from the lung with a half-time of 40 d at a concentration of 0.5 mg/m <sup>3</sup> , at higher concentrations clearance was impaired. Dose-dependent inflammatory response dominated by neutrophils for 1 week exposures and macrophages for 4-week exposures. The inflammatory response correlated better with the surface area dose than mass or volume doses. 5 mg/m <sup>3</sup> was the lowest aerosol concentration at which the early as well as the later inflammatory response was observed.	(Keller et al.,2014) **
Al-doped CeO <sub>2</sub> NPs (NanoCare project)	2-160 (TEM), > 20 × 10 <sup>3</sup> (SEM), 23 (XRD)	46.0	MMAD (μm)/GSD 1.4/2.3, 1.2/2.1, 1.0/2.5;	0.45 ± 0.1, 25.8 ± 1.7 mg/m <sup>3</sup> × 6 h/d × 5 d/wk × 1 wk 0.5 ± 0.2, 5.3 ± 0.9, 25.9 ± 6.0 mg/m <sup>3</sup> × 6 h/d × 5 d/wk × 1 wk;	Wistar rats	1-wk groups - BALF at 3 and 24 d post and histopathology and organ burden at 0 and 21 d post. 4-wk groups - BALF 1 and 35 d post, histopathology at 2 and 34 d post and lung burden at 7 time points to exposures 129 d post	Inhaled CeO <sub>2</sub> NPs cleared from the lung with a half-time of 40 d at a concentration of 0.5 mg/m <sup>3</sup> , at higher concentrations clearance was impaired. Dose-dependent inflammatory response dominated by neutrophils for 1 week exposures and macrophages for 4-week exposures. The inflammatory response correlated better with the surface area dose than mass or volume doses. 5 mg/m <sup>3</sup> was the lowest aerosol concentration at which the early as well as the later inflammatory response was observed.	(Keller et al.,2014) **
CeO <sub>2</sub> NPs (NM-211) (BASF SE);	4-15 (TEM), 12.5 (XRD)	33 (Hg), 53 (BET)	MMAD (μm)/GSD 1.9/2.9, 2.2/2.4	0.48 ± 0.0, 5.2 ± 1.1, 25.6 ± 6.0 mg/m <sup>3</sup> × 6 h/d × 5 d/wk × 4 wks;	Wistar rats	1-wk groups - BALF at 3 and 24 d post and histopathology and organ burden at 0 and 21 d post. 4-wk groups - BALF 1 and 35 d post, histopathology at 2 and 34 d post and lung burden at 7 time points to exposures 129 d post	Inhaled CeO <sub>2</sub> NPs cleared from the lung with a half-time of 40 d at a concentration of 0.5 mg/m <sup>3</sup> , at higher concentrations clearance was impaired. Dose-dependent inflammatory response dominated by neutrophils for 1 week exposures and macrophages for 4-week exposures. The inflammatory response correlated better with the surface area dose than mass or volume doses. 5 mg/m <sup>3</sup> was the lowest aerosol concentration at which the early as well as the later inflammatory response was observed.	(Keller et al.,2014) **
CeO <sub>2</sub> NPs (NM-212) (NanoMile project)	40 (TEM), 3-150 × 10 <sup>3</sup> (SEM), 40.0 (XRD);	30 (Hg), 27 (BET);	MMAD (μm)/GSD 1.6/2.1, 1.3/2.1, 0.9/2.5;	0.48 ± 0.0, 5.2 ± 1.1, 25.6 ± 6.0 mg/m <sup>3</sup> × 6 h/d × 5 d/wk × 4 wks;	Wistar rats	1-wk groups - BALF at 3 and 24 d post and histopathology and organ burden at 0 and 21 d post. 4-wk groups - BALF 1 and 35 d post, histopathology at 2 and 34 d post and lung burden at 7 time points to exposures 129 d post	Inhaled CeO <sub>2</sub> NPs cleared from the lung with a half-time of 40 d at a concentration of 0.5 mg/m <sup>3</sup> , at higher concentrations clearance was impaired. Dose-dependent inflammatory response dominated by neutrophils for 1 week exposures and macrophages for 4-week exposures. The inflammatory response correlated better with the surface area dose than mass or volume doses. 5 mg/m <sup>3</sup> was the lowest aerosol concentration at which the early as well as the later inflammatory response was observed.	(Keller et al.,2014) **
	7.8 (TEM); 10.0 (DLS);	101 (BET)			Fisher 344 rats	3 d, 1 and 3 months post		(Morimoto et al.,2015) **

(continued)

Table 1. Continued.

Characterization of primary particles		Reference			
Primary particle diameter (nm)	Surface area (m <sup>2</sup> /g)	Characterization of aerosols (MMAD – mass median aerodynamic diameter; GSD – geometric standard deviation; CMD – count median diameter; GMD – geometric mean diameter)	Exposure dose (aerosol concentration × exposure duration)		
CeO <sub>2</sub> particles			Animal models		
			Animal sacrifice time points post-exposure		
			Brief biological findings		
CeO <sub>2</sub> NPs (Wako Chemical Ltd)		GMD (nm) 110 ± 12.5 (high dose), 87.6 ± 7.9 nm (low dose)	10.2 ± 1.38 mg/m <sup>3</sup> (high dose) and 2.09 ± 0.29 mg/m <sup>3</sup> (low dose) × 6 h/d × 5 d/wk × 4 wks	CeO <sub>2</sub> NPs (either through inhalation or intratracheal instillation) induced not only acute but also chronic inflammation in the lung.	(* nose-only inhalation; ** whole-body exposure)
CeO <sub>2</sub> NPs (produced in-house)	N/A	GMD (nm) 146 (fresh 1), 195 (fresh 2), 174 (aged 1), 151 (aged 2)	172 (fresh 1), 585 (fresh 2), 483 (aged 1), and 439 (aged 2) µg/m <sup>3</sup> × 4 hrs	The biodistribution of fresh and aged CeO <sub>2</sub> NPs followed the same patterns, with the highest amounts recovered in the faeces and lungs.	(Li et al.,2016) *
CeO <sub>2</sub> NPs (Evonik-Degussa)	56.7	GMD(nm) 372 (high dose), 295 (low dose)	8, 30, 152 mg/m <sup>3</sup> × 60 min	BALF cell analyses revealed both neutrophilic and lymphocytic inflammation to a more persistent inflammation; both neutrophilic and lymphocytic inflammation was seen at 13 weeks post.	(Larsen et al.,2016)**
CeO <sub>2</sub> NPs (produced in-house)	N/A	CMD (nm)/GSD 182 ± 10/1.88	3.98 ± 0.23 mg/m <sup>3</sup> × 3 h/d × 5 d/wk × 4 wks	CeO <sub>2</sub> NPs exposure had no major toxicological effects apart from modest inflammatory histopathology in the lung.	(Dekkers et al.,2017)*
CeO <sub>2</sub> NPs (NM-212) (provided by FH-IME)	27.2 (BET)	MMAD (µm)/GSD 0.71/3.59, 0.63/3.83, 0.68/4.32, 0.79/3.50	0.1, 0.3, 1.0 and 3.0 mg/m <sup>3</sup> × 6h/d × 5d/wk × 1, 28, 90 d	Increasing nanoparticle dose levels and ongoing exposure. CeO <sub>2</sub> NPs penetrate the alveolar space and affect the respiratory tract mainly in terms of dose-dependent inflammation, with post-exposure persistence.	(Schwozter et al.,2017) *
CeO <sub>2</sub> NPs (produced in-house)	N/A	CMD (nm)/GSD 43.4/1.70 (1-wk exposure); 43.8/1.72 (2-wk exposure)	1.8 mg/m <sup>3</sup> × 3 h/d × 4 d/w × 1 wk or 2 wks	Changes in gene expression in AEL cells (30 of 391 genes investigated) indicate that the cells contribute to CeO <sub>2</sub> NP caused inflammatory and oxidative stress reactions in the respiratory.	(Schwozter et al.,2018) *
				Short-term inhalation exposure to nano-sized CeO <sub>2</sub> NP agglomerates induced a significant pulmonary inflammatory effect with a limited resolution by 7 d post-exposure.	The present study



**Table 2.** Summary of aerosol characteristics and deposited dose estimates.

Exposure group	CMD (nm)	GSD	Number conc. (particles/cm <sup>3</sup> )	Mass conc. (mg/m <sup>3</sup> )	Dose (lung) (µg)	Dose (alveolar) (µg)
1-week exposure (3 h/d, 4 d/week)	43.4	1.70	$2.16 \times 10^6$	1.80	79	49
2-week exposure (3 h/d, 4 d/week)	43.8	1.72	$1.96 \times 10^6$	1.82	161	100

agglomerates (Table 1), significantly larger than used in this study, and the resulting effects are typically less marked than indicated here. To achieve similar or relatively comparable toxicological effects, inhalation studies with micron-sized CeO<sub>2</sub>NP aerosols usually used higher aerosol concentrations or longer exposure durations (Table 1). Landsiedel et al. (2014), for example, used a similar short-term repeated exposure study design (6 h/d for 5 d with sacrifice at 3 d) with a micron-sized aerosol, which at the low concentration (0.8 mg/m<sup>3</sup>) delivered a very similar 'exposure dose' (i.e. concentration × duration) to our one week exposure, and yet their results at this concentration indicate a significantly lower response, with small but significant changes for only three endpoints, including neutrophil and lymphocyte number but not LDH. Only at the medium and high concentrations, delivering exposure doses >4 times higher, were significant changes seen, similar to those here. Keller et al. (2014) also used a micron-sized aerosol in a short-term repeated dose study using three concentrations, the lowest of which delivered a similar exposure dose to our 1-week study. However, it was only at the medium and high concentrations, delivering exposure doses >5 times higher than our study, that a broad pattern of changes was seen, similar to the results presented here. It is clearly more difficult to make direct comparisons with the results from studies with longer exposure durations; however, it is instructive to note that levels of CCL2(MCP-1), which were significantly enhanced in this study, were only significantly enhanced in a 28-d study (6 h/d, 5 d/week, 4 weeks) (Schwotzer et al. 2017, 2018) at the two highest concentration levels, which would have resulted in exposure doses >3 times higher than this study, and for neutrophil numbers and LDH levels only the highest concentration (3 mg/m<sup>3</sup>), delivering an exposure dose ~9 times greater, produced similar effects to those reported here. Schwotzer et al. (2018) also assessed the effect of exposure on the expression of 391 genes in alveolar epithelial type II cells and identified significant regulatory changes to a total of 30 genes, many of which (e.g. inflammatory cytokines: CCL2, CCL22, CCL7, and CCL17; markers of lung

cancer: Mmp12, indicators of oxidative stress: Fabp4 and Noxo1) were also identified in this study, but again significant changes to gene regulation were only seen at exposure doses markedly higher than used here.

The above comparison supports a conclusion that nano-sized aerosols of CeO<sub>2</sub>NPs are more effective than micron-sized at generating effects. A few other *in vivo* inhalation studies have used nano-sized CeO<sub>2</sub>NPs aerosols, albeit with larger aerosols than used here (40 nm). For example, Demokritou et al. (2013) used a 90 nm aerosol and a similar study design (2.7 mg/m<sup>3</sup> × 2 h/d × 4 d), resulting in a very similar exposure dose which generated significant neutrophilia and cell damage (LDH), similar to this study. Comparing the two studies, it is possible to argue that the levels of PMN infiltration and LDH are higher in the current study suggesting greater effects for the smaller aerosol; however, this may be a result of other factors including differences in the sacrifice time post-exposure (1 d versus 3 d). Morimoto et al. (2015) used an approximately nano-sized (90–110 nm) aerosol in a 28-d study (2 and 10 mg/m<sup>3</sup>) and found a pattern and degree of inflammatory effects at 3 and 7 d post-exposure similar to the current study despite significantly greater levels of exposure, again suggesting a greater effect for the smaller aerosol particles. It is also interesting to note that Morimoto et al (2015) saw a reduction in effects between 3 and 7 d for some endpoints, which was not seen for our 2-week exposure. The results of our study are, therefore, broadly consistent with the small number of studies using nano-sized aerosols, but suggestive of a greater biological potency for our smaller aerosol.

It is generally understood that aerosol particle size influences the resulting biological effects following inhalation for a number of related reasons: level and pattern of deposition within the lung depends in detail on the aerosol particle size distribution in a non-linear manner, but with aerosol particles below 100 nm (peak around 20 nm) generally depositing more efficiently in the alveolar region than larger particles (Asgharian et al. 2009); smaller

particles may also be less efficiently phagocytosed and, therefore, cleared from the lung than larger particles, thus leading potentially to prolonged exposure and build-up; and smaller particle size also implies a greater surface area per unit deposited mass, which a number of *in vitro* and *in vivo* studies have linked to greater toxicity (e.g. Oberdörster et al. 2005; Stoeger et al. 2006). All these factors may have contributed to the greater apparent short-term toxicity of the aerosols used in this study in comparison with others in the literature.

A generally accepted paradigm is that the toxicity of nanomaterials arises primarily as a result of their ability to generate reactive oxygen species (ROS) and thus oxidative stress damage (Fu et al. 2014). Studies have demonstrated that CeO<sub>2</sub>NPs can induce oxidative stress and resulting toxicity *in vivo* (Nemmar et al. 2017) and *in vitro* (Park et al. 2008b; Eom and Choi 2009). The hierarchical model of oxidative stress (Damoiseaux et al. 2011) proposes that cells and tissues respond to increasing levels of NP-induced oxidative stress via various enzyme systems - mild oxidative stress results in transcriptional activation of phase II antioxidant enzymes via nuclear factor (erythroid-derived 2)-like (Nrf2) induction; and at an intermediate level, redox-sensitive mitogen-activated protein kinase (MAPK) (family includes p38 MAPK and growth factor-regulated extracellular signal-related kinases (ERK)) and nuclear factor kappa-light-chain enhancer of activated B cells (NF-kappaB) cascades mount a pro-inflammatory response. Compatible with this hypothesis, *in vitro* studies have shown that CeO<sub>2</sub>NPs induce toxicity in human bronchial epithelial cells via oxidative stress and the p38-Nrf2 signaling pathway (Eom & Choi 2009) and in human hepatoma cells via oxidative stress and the activation of MAPK signaling pathways (Cheng et al. 2013). One of the significantly enriched terms in the Gene Ontology analysis of the 67 differentially expressed genes in this study (Supplementary Table S2) was GO:0070374 – positive regulation of ERK1 and ERK2 cascade, which is also consistent with the above model. MAPK pathways have also been shown to mediate toxicity for other nanomaterials, e.g. titanium dioxide (Park et al. 2008c) and other inhaled pollutants, e.g. cadmium (Cornet-Boyaka et al. 2012).

### Cerium speciation

Cerium can exist in both 3+ and 4+ oxidation states. Typically the cerium in CeO<sub>2</sub>NPs is predominantly Ce<sup>4+</sup>, however, surface defects mean that Ce<sup>3+</sup> is also found at the surface, and indeed for CeO<sub>2</sub>NPs (3–30 nm) the majority of the surface ceria is Ce<sup>3+</sup> (Deshpande et al. 2005). It has been hypothesized that initial differences in the Ce<sup>3+</sup>/Ce<sup>4+</sup> ratio on the NP surface and changes to this following exposure may play a significant role in toxicity determination (Auffan et al. 2009). In our study, to our knowledge the first to investigate cerium speciation in rat lung after inhalation exposure to CeO<sub>2</sub>NPs, analysis of the XANES cerium spectra (Figure 7) indicates that the cerium in the nanoparticles was largely Ce<sup>4+</sup>; however, the cerium in the tissue samples was 15–21% Ce<sup>3+</sup>, indicating a change in speciation following delivery to the lung. This speciation change is consistent with *in vitro* studies, which have indicated higher Ce<sup>3+</sup> speciation inside rather than outside cells (Szymanski et al. 2015). Some studies have found that the presence of phosphate ions in aqueous systems significantly affects the reactivity of ceria and it has been hypothesized that the formation of cerium phosphate in biological systems would 'trap' cerium in the 3+ state and thus block potential cycling between Ce<sup>3+</sup> and Ce<sup>4+</sup> (Singh et al. 2011). Further studies are required to investigate the potential links between speciation and toxicity mechanisms, especially for long-term pulmonary effects, which, given the ability of CeO<sub>2</sub>NPs to generate ROS in a number of *in vitro* and *in vivo* systems (Lin et al. 2006; Park et al. 2008b; Nemmar et al. 2017) may relate to ROS generation capacity.

### Lipidomic analysis

The most abundant lipid classes in the lung lipiome are glycerophosphocholines (PC), due to their significant role in lung surfactant, glycerophosphoethanolamines (PE), glycerophosphoserines (PS), glycerolphosphoglycerols, and sphingolipids (Titz et al. 2016). Few studies have investigated the effect of inhaled nanomaterials on the lung lipiome and to date, all have been targeted. Gold nanoparticles (3-week exposure) had no effect on total lung surfactant, sphingolipids or glycerophospholipids, except

a decrease in one PS species (Yu et al. 2007). Single-walled carbon nanotubes (4-d exposure) produced no changes in total phospholipids, no oxidized PC or PE species, but some oxidized minor phospholipid species, suggesting selective rather than nonspecific effects (Tyurina et al. 2011). Recently, alterations in numerous phosphorylcholine-containing lipid species were identified in rat lung following inhalation of ZnO particles (35 nm and 250 nm), with the analysis suggesting that these included lipids involved in membrane conformation and cellular signaling (Lee et al. 2016, 2018). In this study, untargeted mass spectrometry-based lipidomics revealed that the most marked effect of CeO<sub>2</sub>NP exposure is the significant increase of some lipids within the category of glycerophospholipids, dominated by PC and PE (Supplementary Tables S3 & S4 and Supplementary File S11). Comparison of the putatively annotated lipids that were perturbed, with information on individual lipid species usually identified within the lung (Griese et al. 2015; Titz et al. 2016; Zemski Berry et al. 2017), revealed that the majority of the perturbed species were not those usually identified at significant concentrations within the lung. Comparing the annotated lipids against a comprehensive profile of lung glycerophospholipids suggests that of the 80 lipids listed by Zemski Berry et al. (2017) only three (PC(14:0/16:0), PC(16:0/16:1) and PE(16:0/18:1)) were significantly modified by CeO<sub>2</sub>NP exposure. The results of the global lipidomics analysis, the first to be undertaken for an *in vivo* nanotoxicology inhalation study, suggest minor changes to a small number of commonly found lipids within the lung, but potentially more marked changes to less abundant lipids, which may indicate effects for specific cells/pathways. This could usefully be investigated further using a targeted analysis of these putatively annotated lipids.

### **Relevance of aerosol concentration and characteristics**

Cerium concentrations in ambient air in Newcastle (UK) post-introduction of Envirox<sup>TM</sup> to local bus fleets were approximately 0.5 ng/m<sup>3</sup> (Park et al. 2008a; Cassee et al. 2011; Gantt et al. 2015). A number of modeling studies have estimated potential future concentrations based on the more extensive

use of the additives, including 1.25 × 10<sup>3</sup> ng/m<sup>3</sup> (HEI 2001), 5–80 ng/m<sup>3</sup> (Park et al. 2008a), and 22 ng/m<sup>3</sup> (Erdakos et al. 2014). These concentrations are lower than used in this study (1.8 × 10<sup>6</sup> ng/m<sup>3</sup>), however, short-term exposures were used rather than the chronic exposures that would arise in the general population from the use of these fuel additives. Ma et al. (2011) estimated a lifetime lung burden of 936 μg/kg and Park et al. (2008a) estimated a 20-year lung burden of 30 μg. The doses delivered in our study were of this order, i.e. comparable to estimated lifetime exposure levels.

Laboratory studies have found ceria particles emitted from various engines using CeO<sub>2</sub>NP fuel additives with a range of sizes, including: majority <80 nm (Skillas et al. 2000); ca. 75 nm (Gantt et al. 2015); and typically 60–300 nm (Dale et al. 2017), all broadly consistent with measurements made during field studies (5–100 nm) (Gantt et al. 2014) and with the size of the aerosol agglomerates used in this study. It is important to note, however, that emitted ceria particles are typically single crystals (or small groups thereof) formed within the engine from the smaller particles (8–10 nm) within the additive, rather than agglomerates as used here. This may impact on the resulting effects and could usefully be investigated further, but in this context it is important to note that studies using a range of sizes of primary particles producing aerosol agglomerates of a similar size have found that the resulting biological effects were very similar at concentrations below overload (Gosens et al. 2014; Keller et al. 2014), suggesting that aerosol particle size, rather than primary particle size, is a key factor driving biological effects. It is also necessary to acknowledge that in the environment some ceria particles would be attached to larger micron-sized soot particles, which may also affect their biological effects, although the importance of this is unclear with one study indicating 40% of ceria particles associated with larger soot particles (Gantt et al. 2015) but another suggesting significantly lower levels (Skillas et al. 2000).

Diesel emissions are complex mixtures of gases and particles, and ultimately a complete assessment of the overall impact of using CeO<sub>2</sub>NP fuel additives on human health needs to consider all aspects of the changes in the emission characteristics (Zhang et al. 2013). Some studies have used diesel exhaust



from machines using fuel additives. Cassee et al. (2012) exposed atherosclerosis-prone mice to exhaust from a diesel engine using standard fuel (DE) or fuel containing CeO<sub>2</sub>NP (DECe) and found a trend of increasing atherosclerotic plaques following DE exposure that was not evident in the DCeE group. Overall there were no clear pathological changes in either group. These results contrast with those of Snow et al. (2014), who exposed rats to diesel exhaust (DE) from a generator run using diesel fuel, with (DECe) and without (DE) the addition of CeO<sub>2</sub>NP and found that DECe induced greater adverse pulmonary effects. Clearly such studies are extremely useful in evaluating the overall effects of the introduction of CeO<sub>2</sub>NP fuel additives, however, the influence of engine type, engine abatement, running conditions, and exhaust ageing may be significant in determining the characteristics of the output. Thus, studies investigating the biological effects of relevant CeO<sub>2</sub>NPs remain of use in understanding their contribution to overall effects.

## Conclusions

Short-term inhalation exposure to nano-sized cerium oxide agglomerates induced a significant pulmonary inflammatory effect with a limited resolution by 7 d post-exposure, indicating the potential for longer-term effects, which is worthy of further investigation. Comparison with the results of previous studies using larger aerosol particle sizes supports a hypothesis that aerosol particle size is a key toxicity driver and thus emphasizes the need for future *in vivo* inhalation studies to use nanomaterial aerosol sizes of environmental relevance.

## Acknowledgements

The authors thank Dr Jennifer Kirwan and Lorraine Wallace (University of Birmingham) for assistance with the multi-omics data collection. Transmission electron microscopy was performed by Mr Lennell Reynolds at the Northwestern University Center for Advanced Microscopy, generously supported by NCI CCSG P30 CA060553 awarded to the Robert H Lurie Comprehensive Cancer Center. The authors thank Diamond Light Source for access to beamline I18 (proposal SP12583-1) that contributed to the results presented here.

## Disclosure statement

The authors report no conflict of interests with the work in this article. The authors alone are responsible for the content and writing of the manuscript.

## Funding

This study was funded by the UK's Natural Environment Research Council and Medical Research Council as part of the FABLE project (From Airborne exposures to BioLogical Effects) (NE/I008314), with support from Public Health England.

## References

- Aalapati, S., S. Ganapathy, S. Manapuram, G. Anumolu, and B. M. Prakya. 2014. "Toxicity and Bio-accumulation of Inhaled Cerium Oxide Nanoparticles in CD1 Mice." *Nanotoxicology* 8 (7): 786–798.
- Asgharian, B., O. Price, F. Miller, R. Subramaniam, F. R. Cassee, J. Freijer, L. Van Bree, and R. De Winter-Sorkina. 2009. MPPD, Multiple-Path Dosimetry Model v2.11. Applied Research Associates (ARA), The Hamner Institutes for Health Sciences, the National Institute of Public Health and the Environment (RIVM), the Netherlands, and the Ministry of Housing, Spatial Planning and the Environment, the Netherlands.
- Auffan, M., J. Rose, T. Orsiere, M. De Meo, A. Thill, O. Zeyons, O. Proux, et al. 2009. "CeO<sub>2</sub> Nanoparticles Induce DNA Damage towards Human Dermal Fibroblasts in Vitro." *Nanotoxicology* 3 (2): 161–171. doi:10.1080/17435390902788086.
- Braakhuis, H. M., F. R. Cassee, P. H. Fokkens, L. J. De La Fonteyne, A. G. Oomen, P. Krystek, W. H. De Jong, H. Van Loveren, and M. V. Park. 2016. "Identification of the Appropriate Dose Metric for Pulmonary Inflammation of Silver Nanoparticles in an Inhalation Toxicity Study." *Nanotoxicology* 10:63–73. doi:10.3109/17435390.2015.1012184.
- Cassee, F. R., A. Campbell, A. J. Boere, S. G. Mclean, R. Duffin, P. Krystek, I. Gosens, and M. R. Miller. 2012. "The Biological Effects of Subacute Inhalation of Diesel Exhaust following Addition of Cerium Oxide Nanoparticles in Atherosclerosis-prone Mice." *Environmental Research* 115: 1–10. doi:10.1016/j.envres.2012.03.004.
- Cassee, F. R., E. C. Van Balen, C. Singh, D. Green, H. Muijser, J. Weinstein, and K. Dreher. 2011. "Exposure, health and Ecological Effects Review of Engineered Nanoscale Cerium and Cerium Oxide Associated with Its Use as a Fuel Additive." *Critical Reviews in Toxicology* 41 (3): 213–229. doi:10.3109/10408444.2010.529105.
- Chen, H.-S., J. Mazzolini, J. Ayers, J. Rappoport, J. Lead, and J. Preece. 2013. Synthesis and characterization of nano ceria for biological applications. Nano-Bio Sensing, Imaging and Spectroscopy SPIE, 7.

- Cheng, G., W. Guo, L. Han, E. Chen, L. Kong, L. Wang, W. Ai, N. Song, H. Li, and H. Chen. 2013. "Cerium Oxide Nanoparticles Induce Cytotoxicity in Human Hepatoma SMMC-7721 Cells via Oxidative Stress and the Activation of MAPK Signaling Pathways." *Toxicology in Vitro* 27 (3): 1082–1088. doi:10.1016/j.tiv.2013.02.005
- Cornet-Boyaka, E., K. Jolivet, A. Bonnegarde-Bernard, J. Rennolds, F. Hassan, P. Mehta, S. Tridandapani, J. Webster-Marketon, and P. N. Boyaka. 2012. "An NF-kappaB-independent and Erk1/2-dependent Mechanism Controls CXCL8/IL-8 Responses of Airway Epithelial Cells to Cadmium." *Toxicological Sciences* 125 (2): 418–429. doi:10.1093/toxsci/kfr310.
- Dale, J., S. Cox, M. Vance, L. Marr, and M. Hochella. 2017. "Transformation of Cerium Oxide Nanoparticles from a Diesel Fuel Additive during Combustion in a Diesel Engine." *Environmental Science & Technology* 51: 1973–1980.
- Damoiseau, R., S. George, M. Li, S. Pokhrel, Z. Ji, B. France, T. Xia, et al. 2011. "No Time to Lose – High Throughput Screening to Assess Nanomaterial Safety." *Nanoscale* 3 (4): 1345–1360. doi:10.1039/c0nr00618a.
- Dekkers, S., M. R. Miller, R. P. F. Schins, I. Romer, M. Russ, R. J. Vandebriel, I. Lynch, et al. 2017. "The Effect of Zirconium Doping of Cerium Dioxide Nanoparticles on Pulmonary and Cardiovascular Toxicity and Biodistribution in Mice after Inhalation." *Nanotoxicology* 11, 794–808. doi:10.1080/17435390.2017.1357214.
- Dekkers, S., T. D. Williams, J. Zhang, J. Zhou, R. J. Vandebriel, L. J. J. De La Fonteyne, E. R. Gremmer, et al. 2018. "Multi-omics Approaches Confirm Metal Ions Mediate the Main Toxicological Pathways of Metal-bearing Nanoparticles in Lung Epithelial A549 Cells." *Environmental Science: Nano* 5: 1506–1517. doi:10.1039/C8EN00071A
- Demokritou, P., S. Gass, G. Pyrgiotakis, J. M. Cohen, W. Goldsmith, W. McKinney, D. Frazer, et al. 2013. "An in Vivo and in Vitro Toxicological Characterisation of Realistic Nanoscale CeO(2) inhalation Exposures." *Nanotoxicology* 7 (8): 1338–1350. doi:10.3109/17435390.2012.739665.
- Deshpande, S., S. Patil, S. V. N. T. Kuchibhatla, and S. Seal. 2005. "Size Dependency Variation in Lattice Parameter and Valency States in Nanocrystalline Cerium Oxide." *Applied Physics Letters* 87 (13): 133113. doi:10.1063/1.2061873.
- Eom, H. J., and J. Choi. 2009. "Oxidative Stress of CeO2 Nanoparticles via p38-Nrf-2 Signaling Pathway in Human Bronchial Epithelial Cell, Beas-2B." *Toxicology Letters* 187 (2): 77–83.
- Erdakos, G. B., P. V. Bhave, G. A. Pouliot, H. Simon, and R. Mathur. 2014. "Predicting the Effects of Nanoscale Cerium Additives in Diesel Fuel on Regional-scale Air Quality." *Environmental Science & Technology* 48 (21): 12775–12782. doi:10.1021/es504050g.
- Fu, P. P., Q. Xia, H.-M. Hwang, P. C. Ray, and H. Yu. 2014. "Mechanisms of Nanotoxicity: Generation of Reactive Oxygen Species." *Journal of Food and Drug Analysis* 22 (1): 64–75. doi:10.1016/j.jfda.2014.01.005.
- Gantt, B., S. Hoque, K. M. Fahey, R. D. Willis, J. M. Delgado-Saborit, R. M. Harrison, K. M. Zhang, et al. 2015. "Factors Affecting the Ambient Physicochemical Properties of Cerium-Containing Particles Generated by Nanoparticle Diesel Fuel Additive Use." *Aerosol Science and Technology* 49 (6): 371–380. doi:10.1080/02786826.2015.1027809.
- Gantt, B., S. Hoque, R. D. Willis, K. M. Fahey, J. M. Delgado-Saborit, R. M. Harrison, G. B. Erdakos, et al. 2014. "Near-road Modeling and Measurement of Cerium-containing Particles Generated by Nanoparticle Diesel Fuel Additive Use." *Environmental Science & Technology* 48 (18): 10607–10613. doi:10.1021/es502169p.
- Geraets, L., A. G. Oomen, J. D. Schroeter, V. A. Coleman, and F. R. Cassee. 2012. "Tissue Distribution of Inhaled Micro- and Nano-sized Cerium Oxide Particles in Rats: Results from a 28-day Exposure Study." *Toxicological Sciences* 127 (2): 463–473. doi:10.1093/toxsci/kfs113.
- Gosens, I., L. E. Mathijssen, B. G. Bokkers, H. Muijser, and F. R. Cassee. 2014. "Comparative Hazard Identification of Nano- and Micro-sized Cerium Oxide Particles Based on 28-day Inhalation Studies in Rats." *Nanotoxicology* 8 (6): 643–653. doi:10.3109/17435390.2013.815814.
- Griese, M., H. G. Kirmeier, G. Liebisch, D. Rauch, F. Stückler, G. Schmitz, R. Zarbock, and I.-B. W. G. O. T. Kids-Lung-Register. 2015. "Surfactant Lipidomics in Healthy Children and Childhood Interstitial Lung Disease." *PLoS One* 10 (2): e0117985. doi:10.1371/journal.pone.0117985.
- HEI 2001. *Evaluation of Human Health Risk from Cerium Added to Diesel Fuel*. Communication 9. Boston, MA: Health Effects Institute (HEI).
- Keller, J., W. Wohlleben, L. Ma-Hock, V. Strauss, S. Groters, K. Kuttler, K. Wiench, et al. 2014. "Time Course of Lung Retention and Toxicity of Inhaled Particles: Short-term Exposure to nano-Ceria." *Archives of Toxicology* 88 (11): 2033–2059. doi:10.1007/s00204-014-1349-9.
- Landsiedel, R., L. Ma-Hock, T. Hofmann, M. Wiemann, V. Strauss, S. Treumann, W. Wohlleben, S. Gröters, K. Wiench, and B. van Ravenzwaay. 2014. "Application of Short-term Inhalation Studies to Assess the Inhalation Toxicity of Nanomaterials." *Particle and Fibre Toxicology* 11: 16.
- Larsen, S. T., P. Jackson, S. S. Poulsen, M. Levin, K. A. Jensen, H. Wallin, G. D. Nielsen, and I. K. Koponen. 2016. "Airway Irritation, inflammation, and Toxicity in Mice following Inhalation of Metal Oxide Nanoparticles." *Nanotoxicology* 10 (9): 1254–1262. doi:10.1080/17435390.2016.1202350.
- Lee, S.-H., T.-Y. Wang, J.-H. Hong, T.-J. Cheng, and C.-Y. Lin. 2016. "NMR-based Metabolomics to Determine Acute Inhalation Effects of Nano- and Fine-sized ZnO Particles in the Rat Lung." *Nanotoxicology* 10 (7): 924–934. doi:10.3109/17435390.2016.1144825.
- Lee, S. H., C. H. Tang, W. Y. Lin, K. H. Chen, H. J. Liang, T. J. Cheng, and C. Y. Lin. 2018. "LC-MS-based Lipidomics to Examine Acute Rat Pulmonary Responses after Nano- and Fine-sized ZnO Particle Inhalation Exposure." *Nanotoxicology* 114: 439–452.
- Li, D., M. Morishita, J. G. Wagner, M. Fatouraie, M. Wooldridge, W. E. Eagle, J. Barres, U. Carlander, C. Emond,

- and O. Jolliet. 2016. "In Vivo Biodistribution and Physiologically Based Pharmacokinetic Modeling of Inhaled Fresh and Aged Cerium Oxide Nanoparticles in Rats." *Particle and Fibre Toxicology* 13 (1): 45.
- Lin, W., Y. W. Huang, X. D. Zhou, and Y. Ma. 2006. "Toxicity of Cerium Oxide Nanoparticles in Human Lung Cancer cells." *International Journal of Toxicology* 25 (6): 451–457.
- Lopez-Ibanez, J., F. Pazos, and M. Chagoyen. 2016. "MBROLE 2.0-functional Enrichment of Chemical Compounds." *Nucleic Acids Research* 44: W201–W204. doi:10.1093/nar/gkw253.
- Ma, J. Y., R. R. Mercer, M. Barger, D. Schwegler-Berry, J. Scabilloni, J. K. Ma, and V. Castranova. 2012. "Induction of Pulmonary Fibrosis by Cerium Oxide Nanoparticles." *Toxicology and Applied Pharmacology* 262 (3): 255–264. doi:10.1016/j.taap.2012.05.005.
- Ma, J. Y., H. Zhao, R. R. Mercer, M. Barger, M. Rao, T. Meighan, D. Schwegler-Berry, V. Castranova, and J. K. Ma. 2011. "Cerium Oxide Nanoparticle-induced Pulmonary Inflammation and Alveolar Macrophage Functional Change in Rats." *Nanotoxicology* 5 (3): 312–325. doi:10.3109/17435390.2010.519835.
- Majestic, B. J., G. B. Erdakos, M. Lewandowski, K. D. Oliver, R. D. Willis, T. E. Kleindienst, and P. V. Bhawe. 2010. "A Review of Selected Engineered Nanoparticles in the Atmosphere: Sources, transformations, and Techniques for Sampling and Analysis." *International Journal of Occupational and Environmental Health* 16 (4): 488–507. doi:10.1179/oeh.2010.16.4.488.
- Morimoto, Y., H. Izumi, Y. Yoshiura, T. Tomonaga, T. Oyabu, T. Myojo, K. Kawai, et al. 2015. "Pulmonary Toxicity of Well-dispersed Cerium Oxide Nanoparticles following Intratracheal Instillation and Inhalation." *Journal of Nanoparticle Research* 17: 442.
- Nemmar, A., P. Yuvaraju, S. Beegam, M. A. Fahim, and B. H. Ali. 2017. "Cerium Oxide Nanoparticles in Lung Acutely Induce Oxidative Stress, Inflammation, and DNA Damage in Various Organs of Mice." *Oxidative Medicine and Cellular Longevity* 2017:12. doi:10.1155/2017/9639035.
- Oberdörster, G., J. Ferin, and B. E. Lehnert. 1994. "Correlation between Particle Size, in Vivo Particle Persistence, and Lung Injury." *Environmental Health Perspectives* 102 (Suppl 5): 173–179. doi:10.1289/ehp.94102s5173.
- Oberdörster, G., A. Maynard, K. Donaldson, V. Castranova, J. Fitzpatrick, K. Ausman, J. Carter, et al. 2005. "Principles for Characterizing the Potential Human Health Effects from Exposure to Nanomaterials: Elements of a Screening Strategy." *Particle and Fibre Toxicology* 2 (1): 8. doi:10.1186/1743-8977-2-8.
- Park, B., K. Donaldson, R. Duffin, L. Tran, F. Kelly, I. Mudway, J. P. Morin, et al. 2008a. "Hazard and Risk Assessment of a Nanoparticulate Cerium Oxide-based Diesel Fuel Additive – a Case Study." *Inhalation Toxicology* 20 (6): 547–566. doi:10.1080/08958370801915309.
- Park, E. J., J. Choi, Y. K. Park, and K. Park. 2008b. "Oxidative Stress Induced by Cerium Oxide Nanoparticles in Cultured BEAS-2B Cells." *Toxicology* 245 (1–2): 90–100. doi:10.1016/j.tox.2007.12.022.
- Park, E. J., J. Yi, K. H. Chung, D. Y. Ryu, J. Choi, and K. Park. 2008c. "Oxidative Stress and Apoptosis Induced by Titanium Dioxide Nanoparticles in Cultured BEAS-2B Cells." *Toxicology Letters* 180 (3): 222–229. doi:10.1016/j.toxlet.2008.06.869.
- Peng, L., X. He, P. Zhang, J. Zhang, Y. Li, J. Zhang, Y. Ma, et al. 2014. "Comparative Pulmonary Toxicity of Two Ceria Nanoparticles with the Same Primary Size." *International Journal of Molecular Sciences* 15 (4): 6072–6085. doi:10.3390/ijms15046072.
- Reed, K., A. Cormack, A. Kulkarni, M. Mayton, D. Sayle, F. Klaessig, and B. Stadler. 2014. "Exploring the Properties and Applications of Nanoceria: Is There Still Plenty of Room at the Bottom?" *Environmental Science: Nano* 1: 390–405. doi:10.1039/C4EN00079J.
- Rice, K. M., S. K. Nalabotu, N. D. Manne, M. B. Kolli, G. Nandyala, R. Arvapalli, J. Y. Ma, and E. R. Blough. 2015. "Exposure to Cerium Oxide Nanoparticles Is Associated with Activation of Mitogen-activated Protein Kinases Signaling and Apoptosis in Rat Lungs." *Journal of Preventive Medicine and Public Health* 48 (3): 132–141. doi:10.3961/jpmph.15.006.
- Schwotzer, D., H. Ernst, D. Schaudien, H. Kock, G. Pohlmann, C. Dasenbrock, and O. Creutzenberg. 2017. "Effects from a 90-day Inhalation Toxicity Study with Cerium Oxide and Barium Sulfate Nanoparticles in Rats." *Particle and Fibre Toxicology* 14: 23.
- Schwotzer, D., M. Niehof, D. Schaudien, H. Kock, T. Hansen, C. Dasenbrock, and O. Creutzenberg. 2018. "Cerium Oxide and Barium Sulfate Nanoparticle Inhalation Affects Gene Expression in Alveolar Epithelial Cells Type II." *Journal of Nanobiotechnology* 16: 16.
- Singh, S., T. Dosani, A. S. Karakoti, A. Kumar, S. Seal, and W. T. Self. 2011. "A Phosphate-dependent Shift in Redox State of Cerium Oxide Nanoparticles and Its Effects on Catalytic Properties." *Biomaterials* 32 (28): 6745–6753. doi:10.1016/j.biomaterials.2011.05.073.
- Skillas, G., Qian, Z., Baltensperger, U., Matter, U. & Burtscher, H., 2000. The Influence of Additives on the Size Distribution and Composition of Particles Produced by Diesel Engines. *Combustion Science and Technology*, 154, 259–273.
- Snow, S. J., J. Mcgee, D. B. Miller, V. Bass, M. C. Schladweiler, R. F. Thomas, T. Krantz, et al. 2014. "Inhaled Diesel Emissions Generated with Cerium Oxide Nanoparticle Fuel Additive Induce Adverse Pulmonary and Systemic Effects." *Toxicological Sciences* 142 (2): 403–417. doi:10.1093/toxsci/kfu187.
- Southam, A. D., R. J. Weber, J. Engel, M. R. Jones, and M. R. Viant. 2017. "A Complete Workflow for High-resolution Spectral-stitching Nanoelectrospray Direct-infusion Mass-spectrometry-based Metabolomics and Lipidomics." *Nature Protocols* 12: 310–328.



- Srinivas, A., P. J. Rao, G. Selvam, P. B. Murthy, and P. N. Reddy. 2011. "Acute Inhalation Toxicity of Cerium Oxide Nanoparticles in Rats." *Toxicology Letters* 205 (2): 105–115.
- Stoeger, T., C. Reinhard, S. Takenaka, A. Schroepfel, E. Karg, B. Ritter, J. Heyder, and H. Schulz. 2006. "Instillation of Six Different Ultrafine Carbon Particles Indicates a Surface Area Threshold Dose for Acute Lung Inflammation in Mice." *Environmental Health Perspectives* 114 (3): 328–333. doi:10.1289/ehp.8266.
- Szymanski, C. J., P. Munusamy, C. Mihai, Y. Xie, D. Hu, M. K. Gilles, T. Tylliszczak, S. Thevuthasan, D. R. Baer, and G. Orr. 2015. "Shifts in Oxidation States of Cerium Oxide Nanoparticles Detected inside Intact Hydrated Cells and Organelles." *Biomaterials* 62: 147–154. doi:10.1016/j.biomaterials.2015.05.042.
- Taylor, N. S., R. Merrifield, T. D. Williams, J. K. Chipman, J. R. Lead, and M. R. Viant. 2016. "Molecular Toxicity of Cerium Oxide Nanoparticles to the Freshwater Alga *Chlamydomonas reinhardtii* Is Associated with Supra-environmental Exposure Concentrations." *Nanotoxicology* 10: 32–41. doi:10.3109/17435390.2014.1002868
- Titz, B., S. Boue, B. Phillips, M. Talikka, T. Vihervaara, T. Schneider, C. Nury, et al. 2016. "Effects of Cigarette Smoke, Cessation, and Switching to Two Heat-Not-Burn Tobacco Products on Lung Lipid Metabolism in C57BL/6 and Apoe<sup>-/-</sup> Mice-An Integrative Systems Toxicology Analysis." *Toxicological Sciences* 149 (2): 441–457. doi:10.1093/toxsci/kfv244.
- Tyurina, Y. Y., E. R. Kisin, A. Murray, V. A. Tyurin, V. I. Kapralova, L. J. Sparvero, A. A. Amoscato, et al. 2011. "Global Phospholipidomics Analysis Reveals Selective Pulmonary Peroxidation Profiles upon Inhalation of Single-Walled Carbon Nanotubes." *ACS Nano* 5 (9): 7342–7353. doi:10.1021/nn202201j.
- Wu, H., A. D. Southam, A. Hines, and M. R. Viant. 2008. "High-throughput Tissue Extraction Protocol for NMR- and MS-based Metabolomics." *Analytical Biochemistry* 372 (2): 204–212.
- Yu, L. E., L.-Y. Lanry Yung, C.-N. Ong, Y.-L. Tan, K. Suresh Balasubramaniam, D. Hartono, G. Shui, M. R. Wenk, and W.-Y. Ong. 2007. "Translocation and Effects of Gold Nanoparticles after Inhalation Exposure in Rats." *Nanotoxicology* 1 (3): 235–242. doi:10.1080/17435390701763108.
- Zemski Berry, K. A., R. C. Murphy, B. Kosmider, and R. J. Mason. 2017. "Lipidomic Characterization and Localization of Phospholipids in the Human Lung." *Journal of Lipid Research* 58 (5): 926–933. doi:10.1194/jlr.M074955.
- Zhang, J., Y. Nazarenko, L. Zhang, L. Calderon, K. B. Lee, E. Garfunkel, S. Schwander, et al. 2013. "Impacts of a Nanosized Ceria Additive on Diesel Engine Emissions of Particulate and Gaseous Pollutants." *Environmental Science & Technology* 47 (22): 13077–13085. doi:10.1021/es402140u.